



Cite this: DOI: 10.1039/d5sc10040b

 All publication charges for this article have been paid for by the Royal Society of Chemistry

Enantioselective synthesis of calix[4]arenes with C–C axial and inherent chirality *via* palladium/chiral norbornene cooperative catalysis

Yiming You,^a Hongwei Cheng,^a Xiao Huang,^a Peng Wang,^c Hengjiang Cong,^{id}^a Hong-Gang Cheng^{id}^{*a} and Qianghui Zhou^{id}^{*ab}

The catalytic asymmetric synthesis of inherently chiral calix[4]arenes, a distinct class of chiral macrocycles with significant applications in asymmetric catalysis, chiral recognition and functional materials, remains a formidable challenge. Moreover, strategies for the simultaneous introduction of multiple stereogenic elements within these scaffolds in a single transformation are highly desirable yet underdeveloped. Herein, we report a one-step protocol that concurrently installs both C–C axial and inherent chirality in a calix[4]arene system through palladium/chiral norbornene (Pd/NBE*) cooperative catalysis. This approach provides direct access to a diverse array of five- and six-membered benzo-fused calix[4]arenes (30 examples) with consistently high enantioselectivity and diastereoselectivity. Notably, the obtained products can be readily transformed into monophosphine ligands bearing both C–C axial and inherent chirality, which exhibit excellent stereocontrol in a silver-catalysed asymmetric [3 + 2] cyclization reaction. Preliminary photophysical and chiroptical studies reveal that these dual-chiral calix[4]arenes exhibit promising g_{lum} factors, demonstrating their potential as versatile chiral scaffolds for advanced organic optoelectronic materials.

Received 22nd December 2025

Accepted 4th March 2026

DOI: 10.1039/d5sc10040b

rsc.li/chemical-science

Introduction

Inherent chirality, a concept introduced by Böhmer in 1994, refers to chirality arising from the asymmetric arrangement of achiral substituents within calix[*n*]arene frameworks.¹ This concept has since been extended to other chiral cyclic architectures that distinguished with conventional central, axial, planar, or helical chirality, including calix[*n*]arenes, saddle-shaped rings, rotaxanes and catenanes, as well as others (Fig. 1A).² Among these, inherently chiral calix[4]arenes constitute a particularly compelling subclass due to their distinctive three-dimensional cavities, which confer significant potential in asymmetric catalysis, chiral recognition, and advanced materials (Fig. 1B).³ Consequently, the development of efficient and stereoselective synthetic routes to these macrocycles has been a central pursuit. Early landmark achievements, such as McKervery's lipase-catalysed

transesterification⁴ and Tsue's Pd-catalysed intramolecular Buchwald–Hartwig amination,⁵ established initial approaches but faced limitations in efficiency or enantiocontrol. A significant advance was achieved by Tong, Wang, and co-workers, who developed a series of effective strategies for the assembly of heteracalix[4]aromatics with high enantioselectivity, including asymmetric intramolecular Buchwald–Hartwig amination, S_NAr reaction, Suzuki–Miyaura coupling and dynamic kinetic resolution (DKR).⁶ More recently, catalytic desymmetrization of prochiral calix[4]arene precursors has emerged as a powerful and efficient route. In 2022, Cai and co-workers developed a Pd-catalysed intramolecular C–H arylation using a chiral phosphine–carboxylate ligand, providing fluorenone-derived calix[4]arenes with a notable luminescence dissymmetry factor (g_{lum}) (Fig. 1C, i-a).⁷ Concurrently, Tong, Wang, and co-workers achieved a Pd/chiral phosphoramidite-catalysed sequential 1,5-palladium migration/intramolecular C–H arylation to construct 9*H*-fluorene-embedded inherently chiral calix[4]arenes (Fig. 1C, i-b).⁸ Recently, Cera, Pirovano *et al.* demonstrated an enantioselective gold(I)-catalysed intramolecular hydroarylation of alkynes, affording phenanthrene-containing calix[4]arenes in high yields and enantioselectivities (Fig. 1C, i-c).⁹ Parallel advances in directed *ortho* C–H functionalization have further enriched the synthetic toolbox. For example, Chen and co-workers developed an elegant amine-directed electrophilic sulfenylation strategy using a chiral sulfide catalyst and hexafluoroisopropanol (Fig. 1C, ii-a).¹⁰ Subsequently, the Yang and

^aHubei Research Center of Fundamental Science-Chemistry, Engineering Research Center of Organosilicon Compounds & Materials (Ministry of Education), Hubei Key Lab on Organic and Polymeric OptoElectronic Materials, College of Chemistry and Molecular Sciences, The Institute for Advanced Studies, Taikang Center for Life and Medical Sciences, State Key Laboratory of Metabolism and Regulation in Complex Organisms, Wuhan University, Wuhan, 430072, China. E-mail: hgcheng@whu.edu.cn; qhzhou@whu.edu.cn

^bSchool of Artificial Intelligence, Wuhan University, Wuhan, 430072, China

^cState Key Laboratory of Coordination Chemistry, School of Chemistry and Chemical Engineering, Nanjing University, Nanjing, 210023, China



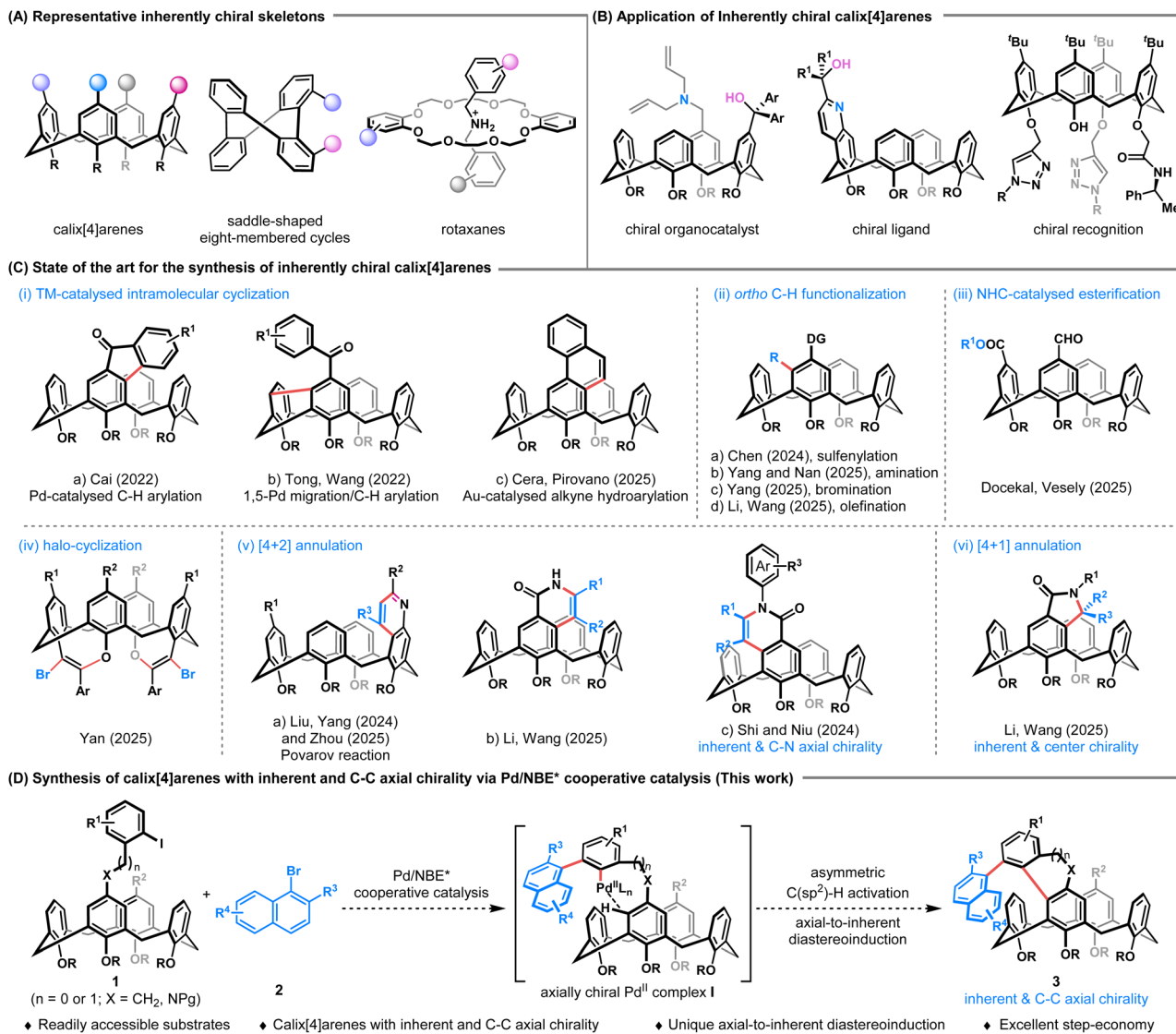


Fig. 1 Catalytic asymmetric approaches to access inherently chiral calix[4]arenes.

Nan groups realized a chiral phosphoric acid (CPA)-catalysed electrophilic aromatic amination or bromination of phenol/amine-decorated calix[4]arenes (Fig. 1C, ii-b, c),¹¹ while Li, Wang and co-workers accomplished a Rh-catalysed *ortho* C-H olefination of calix[4]arene-based carboxamides (Fig. 1C, ii-d).¹² Complementary organocatalytic desymmetrization approaches have also been successfully applied, including NHC-catalysed esterification by Veselý, Dočekal (Fig. 1C, iii)¹³ and Yan's CPA-catalysed enantioselective halo-cyclization (Fig. 1C, iv).¹⁴ Most recently, annulation strategies have proven highly effective for the construction of inherently chiral calix[4]arenes. In this context, Liu, Yang and Zhou independently disclosed a CPA-catalysed Povarov/aromatization sequence (Fig. 1C, v-a).¹⁵ The groups of Niu and Shi concurrently developed a cobalt(III)/Salox-catalysed C-H activation/[4 + 2] annulation with alkynes to simultaneously install both inherent and C-N axial chirality (Fig. 1C, v-c).¹⁶ Li, Wang and co-workers realized a Rh-catalysed *ortho* C-H alkylation followed by intramolecular [4 + 2] annulation (Fig. 1C, v-b), as well as a Rh-catalysed oxidative [4 +

1] annulation with 1,3-enynes to access calix[4]arenes bearing both inherent and central chirality with excellent stereocontrol (Fig. 1C, vi).¹² Despite these impressive advancements, current methodologies remain predominantly focused on the assembly of calix[4]arenes with solely inherent chirality. The concurrent integration of an additional stereogenic element, such as C-C axial chirality, within the same scaffold is largely underdeveloped. Such "dual-chiral" architectures could unlock synergistic functions and novel material properties but pose a formidable synthetic challenge, requiring precise control over multiple stereogenic elements in a single transformation.

Our group has recently demonstrated the power of palladium/chiral norbornene (Pd/NBE*) cooperative catalysis¹⁷ (also known as the asymmetric Catellani reaction¹⁸) to construct atropisomeric *o*-terphenyls with 1,2-diaxes¹⁹ or ferrocenes with both axial and planar chirality,²⁰ guided by axial-to-axial or axial-to-planar diastereoselection, respectively. Inspired by these studies, we envisioned that this catalytic platform could be extended to achieve an unprecedented axial-to-inherent



diastereoselection, enabling the one-step assembly of calix[4]arenes bearing both C–C axial and inherent chirality. As depicted in Fig. 1D, we proposed that in the presence of Pd/NBE* cooperative catalysis, the reaction between readily accessible *ortho*-calix[4]arene-tethered aryl iodide **1** and a bulky β -substituted naphthyl bromide **2** would first generate an axially chiral Pd^{II} complex **I**. This intermediate would then undergo an intramolecular, enantioselective C(sp²)-H activation, where the pre-established axial chirality dictates the formation of the inherent chirality during cyclization, affording the desired dual-chiral product **3**. Given the ready accessibility of the starting materials (**1** and **2**) and the unique axial-to-inherent diastereoselection mode, this strategy provides a highly efficient platform to access calix[4]arenes with both C–C axial and inherent chirality. However, multiple challenges are also associated with this cascade process: (1) competing side reactions such as direct cyclization of **1** or protodepalladation of intermediate **I** must be suppressed and (2) the efficiency of the unprecedented axial-to-inherent diastereoselection is difficult to predict, as it depends critically on controlling the conformational dynamics of the calix[4]arene during the stereo-defining C–H activation step. Herein, we report the successful realization of this strategy, providing a direct, one-step synthetic route to a diverse range of benzo-fused calix[4]arenes bearing

concurrent C–C axial and inherent chirality with high efficiency and excellent stereocontrol.

Results and discussion

To explore this intriguing process, we commenced our study with a model reaction between *ortho*-calix[4]arene-tethered aryl iodide **1a** and methyl 1-bromo-2-naphthoate **2a** (Table 1). Delightfully, under initial conditions using Pd(acac)₂ (10 mol%), TFP (tri(furan-2-yl)phosphine) (10 mol%), (1*R*,4*S*)-2-ethyl ester-substituted norbornene **NBE**^{1*} (99% e.e., 30 mol%), pivalic acid (30 mol%), and Cs₂CO₃ (2.0 equiv.) in toluene (0.1 M) at 80 °C, the desired product **3a** with both C–C axial and inherent chiralities was obtained in 60% yield with excellent enantioselectivity (>99%/99% e.e.) and moderate diastereoselectivity (5:1 d.r.) (entry 1). Switching the palladium precursor from Pd(acac)₂ to Pd(OPiv)₂ enhanced the yield to 71% (entry 2), possibly because the pivalate anion facilitates C–H activation and suppresses competing pathways. Subsequent ligand and **NBE*** screening identified TFP and **NBE**^{1*} as the optimal combination (entries 2–6). Diluting the reaction concentration to 0.05 M further improved the yield to 78% while retaining high stereoselectivity (entry 7). Finally, replacing the naphthoate substrate **2a** with the more sterically hindered diphenylphosphonyl-substituted analogue **2b** afforded product **3b** in 81% isolated yield with

Table 1 Optimization of reaction conditions^a

| Entry | 2 | Pd cat. | L | NBE [*] | Yield ^b (%) | d.r. ^c | e.e. ^d (%) |
|------------------|-----------|-----------------------|------------------|--------------------------|------------------------|-------------------|-----------------------|
| 1 | 2a | Pd(acac) ₂ | TFP | NBE ^{1*} | 60 | 5:1 | >99/99 |
| 2 | 2a | Pd(OPiv) ₂ | TFP | NBE ^{1*} | 71 | 6:1 | >99/99 |
| 3 | 2a | Pd(OPiv) ₂ | XPhos | NBE ^{1*} | 7 | — | — |
| 4 | 2a | Pd(OPiv) ₂ | PPh ₃ | NBE ^{1*} | 65 | 6:1 | >99/99 |
| 5 | 2a | Pd(OPiv) ₂ | TFP | NBE ^{2*} | 61 | 6:1 | >99/99 |
| 6 | 2a | Pd(OPiv) ₂ | TFP | NBE ^{3*} | 5 | — | — |
| 7 ^e | 2a | Pd(OPiv) ₂ | TFP | NBE ^{1*} | 78 | 6:1 | >99/99 |
| 8 ^{e,f} | 2b | Pd(OPiv) ₂ | TFP | NBE ^{1*} | 79 (81) ^g | >19:1 | >99 |

NBE^{1*} (99% e.e.)

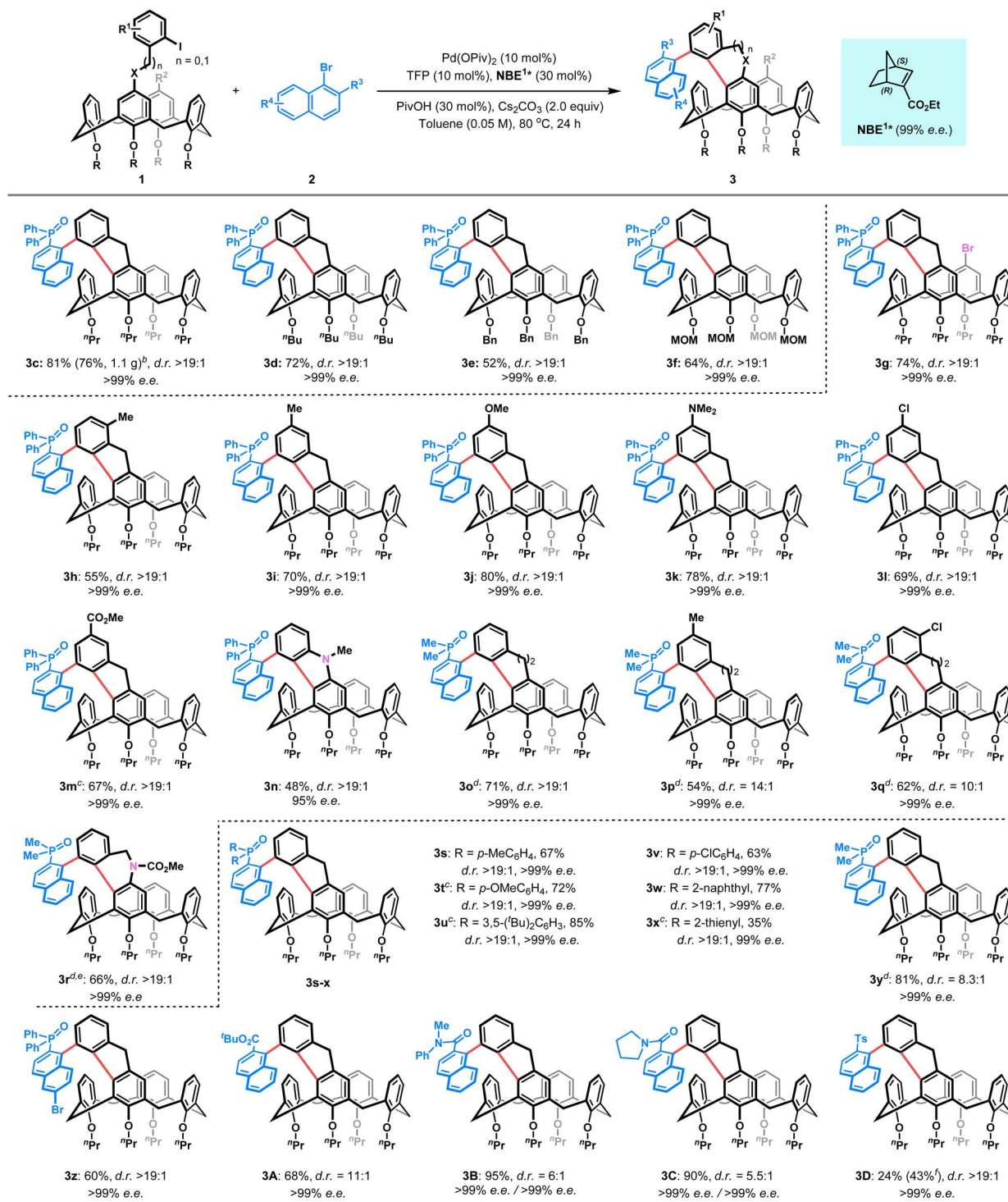
NBE^{2*} (99% e.e.)

NBE^{3*} (97% e.e.)

TFP

XPhos

^a All reactions were performed on a 0.05 mmol scale. ^b The yield was determined by ¹⁹F NMR analysis with 4,4'-difluoro-1,1'-biphenyl as an internal standard. ^c d.r. was determined by crude ¹⁹F NMR analysis. ^d e.e. was determined by chiral HPLC analysis. ^e Toluene (0.05 M) was applied. ^f **2b** (1.6 equiv.) was applied. ^g Isolated yield in parentheses. TFP: tri(furan-2-yl)phosphine.

Table 2 Reaction scope of *ortho*-calix[4]arene-tethered aryl iodides and β -substituted naphthyl bromides^a

^a Reaction conditions: **1** (0.1 mmol, 1.0 equiv.), **2** (0.16 mmol, 1.6 equiv.), Pd(OPiv)₂ (10 mol%), TFP (10 mol%), NBE^{1*} (30 mol%), PivOH (30 mol%), Cs₂CO₃ (2.0 equiv.), and toluene (0.05 M) at 80 °C for 24 h. ^b 1.5 mmol scale. ^c 48 h instead of 24 h. ^d 110 °C instead of 80 °C. ^e 72 h instead of 24 h. ^f Yield based on the recovered starting material.

excellent enantioselectivity (>99% e.e.) and diastereoselectivity (d.r. >19 : 1) (entry 8). Therefore, the reaction conditions listed in entry 8 were established as the optimal ones for this transformation (see Tables S1–S5 for optimization details).

With the optimal reaction conditions established, we first investigated the scope of *ortho*-calix[4]arene-tethered aryl iodide **1**, employing naphthyl bromide **2b** or **2c** as the fixed reaction partner. As shown in Table 2, varying alkoxy groups at the



lower-rim of calix[4]arenes had a minimal impact on stereoselectivity. Substrates **1b–e**, bearing ⁿPr, ⁿBu, Bn or MOM groups, all reacted smoothly to afford the corresponding products **3c–f** in 52–81% yields with >99% e.e. and >19:1 d.r. In addition, halogen functionality was also tolerated, as illustrated by the *para*-bromo-substituted derivative (**1f**), which afforded product **3g** in 74% yield with excellent stereocontrol. Notably, the electronic nature of the aryl iodide tether proved highly adaptable. Aryl iodides with an electron-donating group (e.g., Me, OMe, and NMe₂) or electron-withdrawing group (e.g., F, Cl, and CO₂Me) all proved to be competent substrates, giving the desired products **3b** and **3h–m** in 55–81% yields with >99% e.e. and >19:1 d.r. Moreover, a carbazole-fused calix[4]arene **3n** was furnished in 48% yield with 95% e.e. and >19:1 d.r. using *ortho*-amino substituted aryl iodide **1m** as the substrate. Furthermore, aryl iodides with a longer tether were also suitable for this approach, providing access to six-membered benzo-fused calix[4]arenes **3o–r** in 54–71% yields with >99% e.e. and 10:1 to >19:1 d.r.

We next surveyed the scope of the bulky naphthyl bromide **2**, with **1b** as the fixed coupling partner. A series of 2-diarylphosphinyl-1-naphthyl bromides with either electron-donating substituents (e.g., *p*-Me, *p*-OMe, and 3,5-di-^tBu) or electron-withdrawing substituents (e.g., *p*-Cl) on the aryl rings reacted efficiently to yield products **3s–v** in moderate to good yields (63–85%). Additionally, 2-naphthyl, 2-thienyl and methyl phosphine oxide-substituted naphthyl bromides also served as suitable arylating reagents to provide the corresponding products **3w–y** in 35–81% yields. It is noteworthy that 6-bromo-diphenylphosphine oxide (**3z**) displayed good reactivity as well. Apart from the phosphonyl groups, other functional handles such as esters (**3a** and **3A**), amides (**3B–C**), and a sulfonyl group (**3D**) were all successfully incorporated, affording the desired products in 43–95% yields. Notably, all products in this series were obtained with excellent enantioselectivities (99% e.e.) and

good to excellent diastereoselectivities (5.5:1 to >19:1 d.r.). Importantly, the scalability of this approach was demonstrated by a 1.5 mmol-scale experiment, which provided 1.1 g of **3c** in 76% yield with >99% e.e. and >19:1 d.r., alongside 88% recovery of the NBE^{1*} cocatalyst.

As the obtained calix[4]arenes with both C–C axial and inherent chiralities are versatile intermediates, their synthetic utility is illustrated by follow-up transformations (Fig. 2A). For instance, reduction of **3c** readily afforded the novel phosphine **4**, which was preliminarily validated as an effective chiral ligand in a silver-catalysed asymmetric [3 + 2] cyclization reaction²¹ (Fig. 2B). In addition, nucleophilic substitution of **3c** with benzyl bromide led to the formation of fluorene-fused calix[4]arene **5** as a single diastereomer in 53% yield. Oxidation of **3c** under air in the presence of KOH produced fluorenone-fused calix[4]arene **6** in 92% yield. The absolute configuration of **6** was unambiguously determined *via* X-ray crystallographic analysis (CCDC 2403829). Subsequently, nucleophilic addition of **6** with phenylmagnesium bromide proceeded smoothly to afford fluorenol-fused calix[4]arene **7** as a single diastereomer in 84% yield. Notably, compounds **5** and **7** each integrate three distinct stereogenic elements: axial, inherent and central chirality, with the configuration of newly generated stereocenter being fully controlled by the pre-existing inherent chirality. Finally, lithium–halogen exchange of 3-bromo-5,5'-di-*tert*-butyl-2,2'-bithiophene, followed by the addition to fluorenone **6** and subsequent intramolecular Friedel–Crafts cyclization, provided the dithiophene-fused spirofluorene **8** in 51% yield. This compound exhibits promising circularly polarized luminescence (CPL) properties (*vide infra*).

With these novel calix[4]arenes bearing both C–C axial and inherent chirality in hand, we initially examined the photo-physical properties of compounds **3c**, **3y**, **3p** and **8** using ultraviolet-visible (UV-vis) absorption and photoluminescence spectroscopy. As shown in Fig. 3a, **3c**, **3y**, **3p** and **8** showed



Fig. 2 (A) Follow-up transformations. Reaction conditions: (a) HSiCl₃, Et₃N, toluene, 120 °C; (b) ⁿBuLi, BnBr, THF, 0 °C to r.t.; (c) KOH, air, DMSO, 40 °C; (d) PhMgBr, THF, 0 °C to r.t.; (e) 3-bromo-5,5'-di-*tert*-butyl-2,2'-bithiophene, ⁿBuLi, THF, –78 °C, then AcOH, H₂SO₄, ⁿhexane/DCM, 60 °C. (B) Synthetic application.

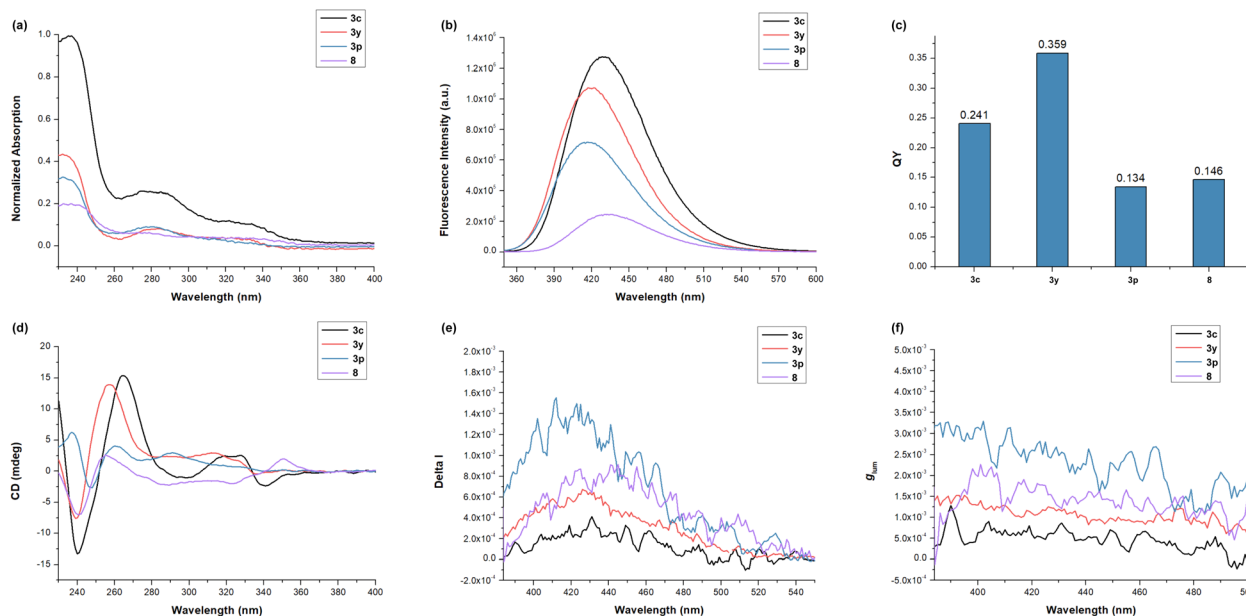


Fig. 3 Investigation of photophysical and chiroptical properties. (a) Absorption spectra of **3c**, **3y**, **3p**, and **8** in DCM (5.0×10^{-5} M). (b) Emission spectra of **3c**, **3y**, **3p**, and **8** in DCM (5.0×10^{-5} M). (c) Quantum yields of **3c**, **3y**, **3p**, and **8** in DCM (5.0×10^{-5} M). (d) CD spectra of **3c**, **3y**, **3p**, and **8** in DCM (5.0×10^{-5} M) at r.t. (e) CPL spectra of **3c**, **3y**, **3p**, and **8** in DCM (5.0×10^{-5} M) at r.t. (f) g_{lum} value–wavelength curves of **3c**, **3y**, **3p**, and **8**.

similar profiles, with strong absorption maxima around 275 nm and weaker features near 320 nm. These compounds displayed clearly broadened fluorescence emission bands, with maxima at 431 nm for **3c**, 420 nm for **3y**, 417 nm for **3p** and 434 nm for **8** (Fig. 3b). Moreover, the quantum yields were determined to be 0.241, 0.359, 0.134, and 0.146 for **3c**, **3y**, **3p**, and **8**, respectively (Fig. 3c). We next explored the chiroptical properties of these compounds *via* circular dichroism (CD) and circularly polarized luminescence (CPL) spectroscopy, respectively. As clearly demonstrated by the CD spectra (Fig. 3d), all these compounds exhibited pronounced Cotton effects ranging from 380 to 550 nm (Fig. 3e). Remarkably, CPL experiments indicated that these compounds were all CPL-active, with compound **3p** displaying the highest luminescence dissymmetry factor (g_{lum}) (3.2×10^{-3} at 411 nm, Fig. 3f), which is comparable to conventional organic small molecules that typically have g_{lum} values ranging from 10^{-5} to 10^{-3} . These results demonstrated the significant potential of dual-chiral calix[4]arene architectures as promising candidates for new chiral organic optoelectronic materials.

Conclusions

In summary, we have developed an efficient strategy to access calix[4]arenes with both C–C axial and inherent chirality *via* Pd/NBE* cooperative catalysis. In this intriguing cascade protocol, the initially introduced axial chirality is orchestrated by Pd/NBE* cooperative catalysis, whereas the subsequent inherent chirality is controlled by the preinstalled axial chirality through an unprecedented axial-to-inherent diastereoselection process. Using this approach, a diverse range of five- and six-membered benzo-fused calix[4]arenes bearing both C–C axial and inherent chirality were synthesized in a single step with excellent

enantioselectivity and diastereoselectivity. These dual-chiral products were readily transformed into new monophosphine ligands, which demonstrated outstanding stereocontrol in a silver-catalysed asymmetric [3 + 2] cyclization reaction. Furthermore, photophysical and chiroptical characterization disclosed promising g_{lum} values for these compounds, highlighting their significant potential in developing new chiral organic optoelectronic materials.

Author contributions

H.-G. Cheng and Q. Zhou conceived the idea and directed the project. Y. You, H. Cheng, X. Huang and P. Wang performed the experiments under the supervision of H.-G. Cheng and Q. Zhou. H. Cong performed the X-ray crystallographic analysis. Y. You, H.-G. Cheng and Q. Zhou co-wrote the manuscript. All authors discussed the results and commented on the manuscript.

Conflicts of interest

There are no conflicts to declare.

Data availability

The supporting data have been provided as part of the supplementary information (SI). Supplementary information: optimization studies, experimental procedures, supporting experimental results, and complete characterization data for all new compounds. See DOI: <https://doi.org/10.1039/d5sc10040b>.

CCDC 2403829 contains the supplementary crystallographic data for this paper.²²

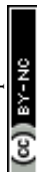


Acknowledgements

This work was supported by the National Key Research and Development Program of China (No. 2022YFA1503703), the National Natural Science Foundation of China (No. 22325106 and 22471204), the Fundamental and Interdisciplinary Disciplines Breakthrough Plan of the Ministry of Education of China (No. JYB2025XDXM402) and the Taikang Center for Life and Medical Sciences of Wuhan University. We thank Prof. W.-B. Liu (WHU) for sharing the instruments, and Mr W. Yuan and Prof. Z. Li (WHU) for their kind assistance with the fluorescence quantum yield measurements.

Notes and references

- V. Böhmer, D. Kraft and M. Tabatabai, *J. Inclusion Phenom.*, 1994, **19**, 17–39.
- (a) J.-W. Han, J.-X. Chen, X. Li, X.-S. Peng and H. N. C. Wong, *Synlett*, 2013, **24**, 2188–2198; (b) E. M. G. Jamieson, F. Modicom and S. M. Goldup, *Chem. Soc. Rev.*, 2018, **47**, 5266–5311; (c) G. Wu, Y. Liu, Z. Yang, T. Jiang, N. Katakam, H. Rouh, L. Ma, Y. Tang, S. Ahmed, A. U. Rahman, H. Huang, D. Unruh and G. Li, *Natl. Sci. Rev.*, 2019, **7**, 588–599; (d) Y. Liu, G. Wu, Z. Yang, H. Rouh, N. Katakam, S. Ahmed, D. Unruh, Z. Cui, H. Lischka and G. Li, *Sci. China: Chem.*, 2020, **63**, 692–698; (e) M. Tang and X. Yang, *Eur. J. Org. Chem.*, 2023, **26**, e202300738; (f) J. Feng, L.-L. Xi and R.-R. Liu, *Chem.–Eur. J.*, 2025, **31**, e02247; (g) J. Feng, L.-L. Xi and R.-R. Liu, *Trends Chem.*, 2025, **7**, 567–570; (h) K. Zhu, D. R. Spring, B.-F. Shi and F. Zhang, *Chem. Soc. Rev.*, 2025, **54**, 10856–10879; (i) W. Qin and G. Cera, *Chem. Rec.*, 2025, **25**, e202400237.
- (a) M. Durmaz, S. Alpaydin, A. Sirit and M. Yilmaz, *Tetrahedron: Asymmetry*, 2007, **18**, 900–905; (b) S. Shirakawa, T. Kimura, S.-i. Murata and S. Shimizu, *J. Org. Chem.*, 2009, **74**, 1288–1296; (c) S.-Y. Li, Y.-W. Xu, J.-M. Liu and C.-Y. Su, *Int. J. Mol. Sci.*, 2011, **12**, 429–455; (d) P. Nandi, A. Solovyov, A. Okrut and A. Katz, *ACS Catal.*, 2014, **4**, 2492–2495; (e) G. E. Arnott, *Chem.–Eur. J.*, 2018, **24**, 1744–1754; (f) P. Lhoták, *Org. Biomol. Chem.*, 2022, **20**, 7377–7390.
- J. K. Browne, M. A. McKervey, M. Pitarch, J. A. Russell and J. S. Millership, *Tetrahedron Lett.*, 1998, **39**, 1787–1790.
- K. Ishibashi, H. Tsue, H. Takahashi and R. Tamura, *Tetrahedron: Asymmetry*, 2009, **20**, 375–380.
- (a) S. Tong, *Acc. Chem. Res.*, 2025, **58**, 3574–3591; (b) S. Tong, J.-T. Li, D.-D. Liang, Y.-E. Zhang, Q.-Y. Feng, X. Zhang, J. Zhu and M.-X. Wang, *J. Am. Chem. Soc.*, 2020, **142**, 14432–14436; (c) Y.-F. Jiang, S. Tong, J. Zhu and M.-X. Wang, *Chem. Sci.*, 2024, **15**, 12517–12522; (d) X.-C. Li, Y. Cheng, X.-D. Wang, S. Tong and M.-X. Wang, *Chem. Sci.*, 2024, **15**, 3610–3615; (e) Q.-L. Lu, X.-D. Wang, S. Tong, J. Zhu and M.-X. Wang, *ACS Catal.*, 2024, **14**, 5140–5146.
- Y.-Z. Zhang, M.-M. Xu, X.-G. Si, J.-L. Hou and Q. Cai, *J. Am. Chem. Soc.*, 2022, **144**, 22858–22864.
- X. Zhang, S. Tong, J. Zhu and M.-X. Wang, *Chem. Sci.*, 2023, **14**, 827–832.
- (a) G. Giovanardi, G. Scarica, V. Pirovano, A. Secchi and G. Cera, *Org. Biomol. Chem.*, 2023, **21**, 4072–4083; (b) M. Goudarzi, A. Alagiyawanna, A. Serafino, S. Rizzato, F. Bertocchi, F. Terenziani, S. Santoro, W. Qin, G. Cera and V. Pirovano, *Chem. Commun.*, 2025, **61**, 16380–16383.
- X.-Y. Zhang, D. Zhu, R.-F. Cao, Y.-X. Huo, T.-M. Ding and Z.-M. Chen, *Nat. Commun.*, 2024, **15**, 9929.
- (a) M. Yuan, W. Xie, S. Yu, T. Liu and X. Yang, *Nat. Commun.*, 2025, **16**, 3943; (b) X. Gong, L. Zhang, X. Liu, M. Shi, M. Zhang, T. Yao, Q. Yan and J. Nan, *Org. Lett.*, 2025, **27**, 12991–12996; (c) M. Yuan, W. Xie and X. Yang, *Chin. Chem. Lett.*, 2025, DOI: [10.1016/j.cclet.2025.112157](https://doi.org/10.1016/j.cclet.2025.112157).
- Y. Yao, F. Wang, X.-X. Li, R. Mi and X. Li, *Angew. Chem., Int. Ed.*, 2025, **64**, e202520283.
- V. Dočekal, L. Lóška, A. Kurčina, I. Císařová and J. Veselý, *Nat. Commun.*, 2025, **16**, 4443.
- L. Peng, Y. Chang, S. Tong, W. Qin, G. Cera and H. Yan, *Angew. Chem., Int. Ed.*, 2025, **64**, e202518659.
- (a) Y.-K. Jiang, Y.-L. Tian, J. Feng, H. Zhang, L. Wang, W.-A. Yang, X.-D. Xu and R.-R. Liu, *Angew. Chem., Int. Ed.*, 2024, **63**, e202407752; (b) S. Yu, M. Yuan, W. Xie, Z. Ye, T. Qin, N. Yu and X. Yang, *Angew. Chem., Int. Ed.*, 2024, **63**, e202410628; (c) X.-Y. Fan, Q.-X. Li, T.-Y. Zhai, S.-F. Ni, G. Wu, L.-W. Ye and B. Zhou, *ACS Catal.*, 2026, **16**, 818–830.
- (a) T. Li, Y. Zhang, C. Du, D. Yang, M.-P. Song and J.-L. Niu, *Nat. Commun.*, 2024, **15**, 7673; (b) P.-F. Qian, G. Zhou, J.-H. Hu, B.-J. Wang, A.-L. Jiang, T. Zhou, W.-K. Yuan, Q.-J. Yao, J.-H. Chen, K.-X. Kong and B.-F. Shi, *Angew. Chem., Int. Ed.*, 2024, **63**, e202412459; (c) L. Zhang, C. Yang, X. Wang, T. Yang, D. Yang, Y. Dou and J.-L. Niu, *Green Chem.*, 2024, **26**, 10232–10239.
- (a) R. Li, F. Liu and G. Dong, *Org. Chem. Front.*, 2018, **5**, 3108–3112; (b) H. Shi, A. N. Herron, Y. Shao, Q. Shao and J.-Q. Yu, *Nature*, 2018, **558**, 581–585; (c) Z.-S. Liu, Y. Hua, Q. Gao, Y. Ma, H. Tang, Y. Shang, H.-G. Cheng and Q. Zhou, *Nat. Catal.*, 2020, **3**, 727–733; (d) Q. Feng, X. Ma, W. Bao, S.-J. Li, Y. Lan and Q. Song, *CCS Chem.*, 2021, **3**, 377–387; (e) Y. Hua, Z.-S. Liu, P.-P. Xie, B. Ding, H.-G. Cheng, X. Hong and Q. Zhou, *Angew. Chem., Int. Ed.*, 2021, **60**, 12824–12828; (f) Z.-S. Liu, P.-P. Xie, Y. Hua, C. Wu, Y. Ma, J. Chen, H.-G. Cheng, X. Hong and Q. Zhou, *Chem*, 2021, **7**, 1917–1932; (g) B. Ding, Q. Xue, H. Wei, J. Chen, Z.-S. Liu, H.-G. Cheng, H. Cong, J. Tang and Q. Zhou, *Chem. Sci.*, 2024, **15**, 7975–7981; (h) Q. Tian, J. Ge, Y. Liu, X. Wu, Z. Li and G. Cheng, *Angew. Chem., Int. Ed.*, 2024, **63**, e202409366; (i) J. Ye, Y. You, D. Xu, S. Deng, L. Qi, C. Liu, C.-C. Liu, H. Cong, P. Wang, H.-G. Cheng and Q. Zhou, *CCS Chem.*, 2025, **7**, 3025–3035; (j) Q. Tian, J. Ge, Y. Liu, X. Wu, Z. Li and G. Cheng, *Org. Lett.*, 2025, **27**, 121–128; (k) Z. Cui, H.-G. Cheng and Q. Zhou, *ChemCatChem*, 2025, **17**, e202500560; (l) L. Li, J. Ye, L. Zhao, L. Zhou, S. Deng, D. Wang, Y. Zhang, H. Cong, Q. Zhou and H.-G. Cheng, *J. Am. Chem. Soc.*, 2025, **147**, 39721–39731.
- (a) M. Catellani, F. Frignani and A. Ragoni, *Angew. Chem. Int. Ed. Engl.*, 1997, **36**, 119–122; (b) J. Ye and M. Lautens, *Nat. Chem.*, 2015, **7**, 863–870; (c) N. Della Ca', M. Fontana, E. Motti and M. Catellani, *Acc. Chem. Res.*, 2016, **49**, 1389–



- 1400; (d) H.-G. Cheng, S. Chen, R. Chen and Q. Zhou, *Angew. Chem., Int. Ed.*, 2019, **58**, 5832–5844; (e) J. Wang and G. Dong, *Chem. Rev.*, 2019, **119**, 7478–7528; (f) K. Zhao, L. Ding and Z. Gu, *Synlett*, 2019, **30**, 129–140; (g) S. Dong and X. Luan, *Chin. J. Chem.*, 2021, **39**, 1690–1705.
- 19 Q. Gao, C. Wu, S. Deng, L. Li, Z.-S. Liu, Y. Hua, J. Ye, C. Liu, H.-G. Cheng, H. Cong, Y. Jiao and Q. Zhou, *J. Am. Chem. Soc.*, 2021, **143**, 7253–7260.
- 20 (a) Y. An, X.-Y. Zhang, Y.-N. Ding, Y. Li, X.-Y. Liu and Y.-M. Liang, *Org. Lett.*, 2022, **24**, 7294–7299; (b) J. Ye, L. Li, Y. You, C. Jiao, Z. Cui, Y. Zhang, S. Jia, H. Cong, S. Liu, H.-G. Cheng and Q. Zhou, *JACS Au*, 2023, **3**, 384–390.
- 21 C.-J. Wang, Z.-Y. Xue, G. Liang and Z. Lu, *Chem. Commun.*, 2009, 2905–2907.
- 22 CCDC 2403829: Experimental Crystal Structure Determination, 2026, DOI: [10.5517/ccdc.csd.cc2lpcwk](https://doi.org/10.5517/ccdc.csd.cc2lpcwk).

